J. Appl. Res. Ind. Eng. Vol. 5, No. 1 (2018) 1–9

Journal of Applied Research on Industrial Engineering
www.journal-aprie.com

An Optimized Heat Sink for ThermoPhotovoltaic Panels

Giampietro Fabbri [1*], ***Matteo Greppi*** [2]
[1]*D.I.N. University of Bologna, Viale Risorgimento 2, 40136 Bologna, Italy.*
[2] *CIRI Aeronautica, University of Bologna, Via Fontanelle 40, 47121 Forli, Italy.*

PAPER INFO

Chronicle:
Received: 10 October 2017
Accepted: 12 February 2018

Keywords:
Solar Panel.
Heat sink.
Thermal Efficiency.
Genetic Algorithm.

ABSTRACT

In the present work, an innovative hybrid solar panel is proposed, which can be used to pave floors or to cover roofs. A particular heat sink is employed, which gives robustness to the panel and provides a better heat transfer effectiveness with respect to tube heat exchangers. The geometry of the heat sink which is employed in the panel is optimized with the help of a numerical model and a genetic algorithm. Some optimization examples are shown. The velocity and temperature distributions on the heat sink cross section are also investigated. The presented hybrid panel allows till 20% increase in the electrical efficiency with respect to a simple photovoltaic panel. Moreover, it can be easily installed under every environmental conditions due to its robustness and resistance to water infiltration.

1. Introduction

A huge amount of solar energy renewable potential is still wasted in most diffused solar panels, due to the low solar to electrical energy conversion efficiency. Despite the recent update, not more than 25 % efficiency is obtained by the commercial photovoltaic cell design as shown by Green [1], and Polman [2]. By improving the overall conversion efficiency of the panels, it is possible to collect most of the wasted heat and achieve a large increase in solar cell efficiency.

Photovoltaic Thermal (PVT) collectors (also called hybrid solar panels) are devices that allow the direct transformation of solar radiation on the same surface into both electrical and thermal energy. Such panels usually present a higher solar to electrical energy conversion efficiency than simply photovoltaic panels. They are therefore one of the best choices in order to lighten the load of thermoelectric distribution networks increasingly subject to excessive stress conditions, to avoid transmission losses, and to reduce carbon emissions [3]. A lot of parameters affect PVT performance (both electrical and thermal) such as the absorption factor [4, 5], the presence of the cover [6], the optimization of the absorber plate parameters (i.e. tube spacing, tube diameter, fin thickness, etc.) [7], the mass flow rate of the heat transferring fluid [8], and the absorber to fluid thermal conductance and configuration design types as shown by Zondag [9, 10] and Tiwari [11]. In the present work, we propose a new kind of hybrid solar panel, which can be used as a tile to pave driveways, areas, and terraces or to cover roofs due to its particular robustness and compactness. Such a panel is covered by two different resins that protect it from atmospheric agents and provide a good thermal insulation. A compact heat exchanger transfers

* Corresponding author
Email: giampietro.fabbri@unibo.it
DOI: 10.22105/jarie.2018.108774.1026

the heat captured by the photovoltaic cells to a water flow. The present work is aimed to analyze and optimize the performance of the heat exchanger with the help of a modified numerical model and a genetic algorithm [12-30] previously developed for other research works [31-33]. The dependence of the heat transfer effectiveness on the number, the diameter, and the distance of the heat exchanger channels is investigated, taking the hydraulic resistance into account, in order to obtain useful information to project a practical hybrid solar panel prototype.

Nomenclature

W_s	total water volume flow rate [m^3/s].
T_f	fluid temperature [K].
T_s	solid temperature [K].
T_b	bulk temperature [K].
T_{max}	maximum temperature [K].
c_p	specific heat capacity at constant pressure [J/(Kg K)].
k_f	fluid thermal conductivity [W/(m K)].
h	global heat transfer coefficient [W/(m K)].
a, c	heat sink margins [m].
b	heat sink internal height [m].
d	heat sink total height [m].
e	distance between channel center z direction [m]
D	channel diameter [m].
N	channel number.
u	fluid velocity [m/s].
u_{max}	maximum fluid velocity [m/s].
Greek symbols	
μ	dynamic viscosity [Pa s].
ρ	density [Kg/m^3].
Dimensionless numbers	
ξ	normalized hydraulic resistance.
Nu_e	equivalent Nusselt number.

2. Hybrid Solar Panel

The proposed hybrid solar panel is composed of a layer of high efficiency mono-crystalline photovoltaic cells that is placed on an aluminum heat sink (Fig. 1). The cells are soldered together and then mechanically connected to the heat sink through a thermally conductive paste, which ensures a satisfactory thermal contact.

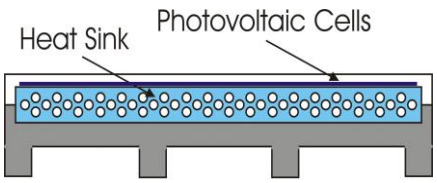

Fig. 1. Section of the hybrid solar panel.

The heat sink consists of an aluminium block with internal parallel channels that is disposed in staggered rows as shown in Fig.1 and Fig. 2. An inlet and an outlet plenum have also been created in the aluminium block. A water flow passes through the channels, absorbing the heat captured by the cell layer.

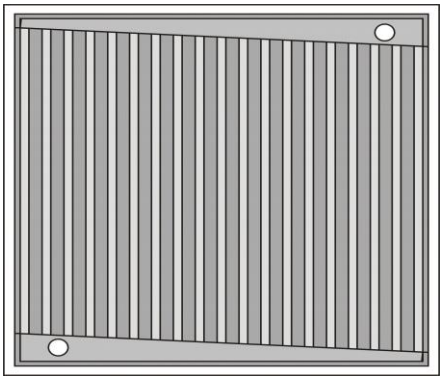

Fig. 2. Section of the heat sink.

The photovoltaic cells and the heat sink are all enclosed in an epoxy resin case, which are obtained by cold polymerization. The upper cover that is obtained by a transparent resin allows the solar radiation to effect on the cells, while the lower cover that is made of an opaque resin avoids heat losses though radiation. Both resins ensure a good mechanical strength and thermal insulation to the entire hybrid panel. The inlet and outlet plena of the heat sink are joined to fast connectors, which ensure a rapid link to the plant tubes. The hydraulic and electrical connectors are integrated into the lower resin case. In order to investigate the performance of such a heat sink, a mathematical model has been created which is able to reproduce the thermal and fluid dynamical alterations induced by changes in channel geometry and disposition. To optimize the efficiency of the heat exchanger, a genetic algorithm that is adapted from a previous work [32] has been employed.

3. Heat Sink Model

The mathematical model of the heat exchanger has been created by introducing some simplifications. The inlet and outlet phenomena have been considered negligible with respect to the heat transfer in the fully developed region of the channels. Moreover, the analysis has been focused on the central area of the heat sink cross section. Letting x and y be the coordinate in the water flow direction and along the least dimension of the aluminium plate, respectively, and supposing that the channel cross section is symmetrical in the z direction, then the dynamic and thermal behaviour of the heat sink cross section central area is symmetrical in the z direction. The analysis has therefore been limited to the cross section side that is between two adjacent symmetry axes, as shown in Fig. 3.

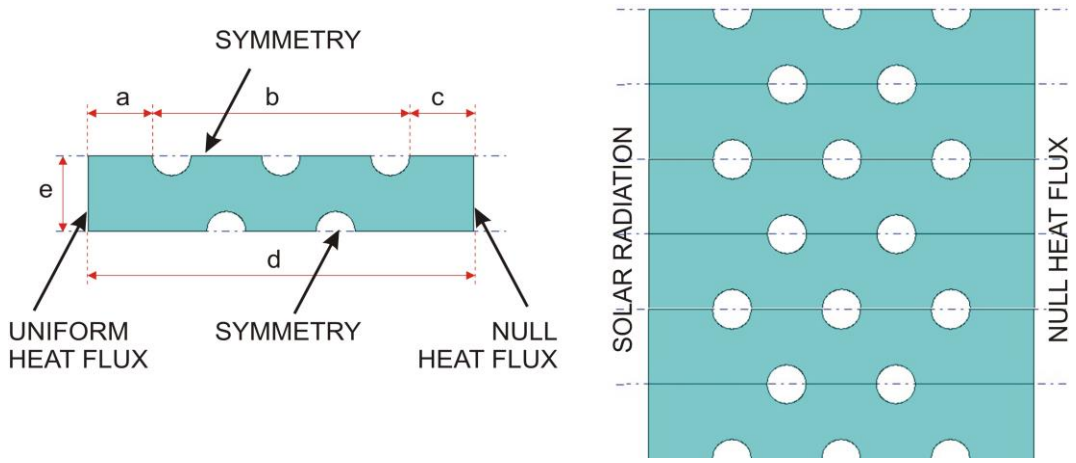

Fig. 3. The investigated domain.

A boundary condition of uniformly imposing heat flux has been considered on the surface in contact with the photovoltaic cells, while null heat flux has been assumed through the opposite side. The following hypotheses have then been introduced:

- The system is at steady state.
- Velocity and temperature profiles are fully developed.
- Fluid and solid properties are uniform and temperature independent.
- Viscous dissipation within the fluid is negligible.
- Natural convection is negligible in comparison with forced convection.

The conditions of fully developed velocity and temperature profiles are approximated only at the centre of the heat sink, far from the inlet and outlet tube regions and from lateral areas. A more accurate analysis could be performed by utilizing a three dimensional model that reproduces the whole heat sink, but such a model could require long calculation times and could not be suitable for the adopted optimization technique. However, it is reasonable to think that the channel geometries, which allow larger increases in the heat transfer at the sink centre, also improve the performance in the peripheral area. Such an assumption should be validated in a subsequent experimental analysis. Under the conditions that were introduced above, the coolant flow is described by the momentum equation:

$$\frac{\partial^2 u}{\partial y^2} + \frac{\partial^2 u}{\partial z^2} = \frac{1}{\mu}\frac{\partial p}{\partial x}\,, \tag{1}$$

where $\boldsymbol{u}$ is the fluid velocity, $\boldsymbol{p}$ is the generalized pressure, which includes the gravitation potential, and $\boldsymbol{\mu}$ is the dynamic viscosity. Eq.(1) must be integrated by imposing, as boundary conditions, that on the contact surface between the fluid and the solid wall, the velocity is zero and on the symmetry axes, the velocity derivative with respect to the axis normal is zero. In the fluid, the temperature $\boldsymbol{T_f}$ must satisfy the following energy balance:

$$\frac{\partial^2 T_f}{\partial y^2} + \frac{\partial^2 T_f}{\partial z^2} = \frac{\rho c_p}{k_f} u \frac{\partial T_f}{\partial x}\,, \tag{2}$$

where $\boldsymbol{\rho}$, $\boldsymbol{c_p}$ and $\boldsymbol{k_f}$ are the density, specific heat, and thermal conductivity of the fluid, respectively. In the solid, the temperature $\boldsymbol{T_s}$ must satisfy the following energy equation:

$$\frac{\partial^2 T_s}{\partial y^2} + \frac{\partial^2 T_s}{\partial z^2} = 0. \tag{3}$$

Equations (2-3) must be integrated by imposing the temperature value at least in one point of the section, a uniformly imposed heat flux through the surface in contact with the photovoltaic cell, and null heat flux through the opposite side and the symmetry planes. The system of Equations (1-3) has been numerically integrated by using the method that was described by Fabbri in [32]. A temperature value has been imposed one point on the surface where the heat flux is applied. After having the determined velocity and temperature distributions, the bulk temperature, global heat transfer coefficient, equivalent Nusselt number $\boldsymbol{Nu_e}$, and normalized hydraulic resistance $\boldsymbol{\xi}$ have been calculated as defined in [32]. In particular, the equivalent Nusselt number is the Nusselt number, which would be obtained if the same heat flux is removed by the heat sink that was dissipated in a flat wall channel of the same height.

$$\mathrm{Nu}_e = \frac{h \cdot 2d}{k_f}, \tag{4}$$

where $\boldsymbol{h}$ is the global heat transfer coefficient and $\boldsymbol{d}$ is the heat sink height. The normalized hydraulic resistance $\boldsymbol{\xi}$ is the ratio between the hydraulic resistance of the whole dissipation section and that of a flat channel of the same height.

$$\xi = \frac{\frac{-dp/dx}{(W_s/e)}}{\frac{12\mu}{d^3}} \quad , \tag{5}$$

where W_s is the total water volume flow rate through the investigate section of the heat sink and e is the height of the section in the z direction.

4. Numerical Analysis

The mathematical model has been employed inside a genetic algorithm [31] in order to optimize the heat sink geometry. In particular, populations of 10 samples have been considered in the genetic algorithm. The 50 % out of the samples having the best effectiveness, which were selected and reproduced. The parameters of the new samples were obtained by copying those of a single parent and introducing 20 % to 50% changes. The algorithm was stopped after no parameter change was observed for 50 generations. Since the aim of the work is to propose a simple practical prototype of the presented innovative hybrid solar panel, the channel section that has been assumed circular; though the mathematical model is able to reproduce the behaviour of more complex symmetrical cross section channels. Moreover, channels have been considered equally spaced in the y direction for all the available length (***b***), i.e. all the heat sink height (***d***) minus some external margins (***a*** and ***c***). The genetic algorithm has then been used under different constraint conditions to find the best combinations of the following parameters: channel number (***N***) in the section part, channel diameter (***D***), distance between channel centre in the ***z*** direction (***e***). A first optimization has been performed by imposing no constrain to the optimized parameters and setting ***a***, ***b***, and ***c*** equal to 5 mm, 20 mm, and 5 mm, respectively. Moreover, the thickness of the aluminium septum between two adjacent channels in the ***y*** or ***z*** direction has been imposed to ideally be not less than 0.1 mm. Under such a condition, the genetic algorithm tended to set an increasingly higher number of channel with an increasingly smaller diameter. Subsequent optimization have then been carried out by constraining the channel diameter to not be smaller than a fixed value or the hydraulic resistance do not exceed an established limit. In Fig. 4, the geometries have been obtained by constraining the channel diameter to be not smaller than 1 mm, 2 mm, and 3 mm. The values of Nu_e and ξ are also reported. All parameters are reported in Table 1 together with those of the subsequent optimizations.

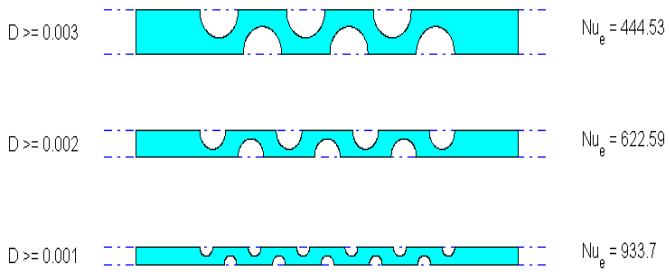

Fig. 4. Obtained optimum geometries by constraining the channel diameter (be not smaller than 1, 2, and 3 mm).

It is evident that higher values of Nu_e are accompanied by larger values of ξ. In the investigated cases, a 100 % and a 150 % increase in the channel diameter cause 33.3 % and 52.4 % reduction in Nu_e, and 85.2 % and 94.3 % reduction in ξ, respectively. Moreover, the obtained optimum geometries are the compromise between the exigency of setting additional channels to enhance the convection and that of having larger septa between the channels to improve the conduction. In Fig. 5, the normalized velocity ($\mathbf{u}/\mathbf{u}_{max}$) and temperature (($\mathbf{T}- \mathbf{T}_b$) / ($\mathbf{T}_{max}-\mathbf{T}_b$)) distributions are shown for the best geometry with

diameter not higher than 3 mm**.** The velocity profile is parabolic as expected for the laminar flow in a circular channel. The temperature distribution is consistent with the imposed boundary conditions.

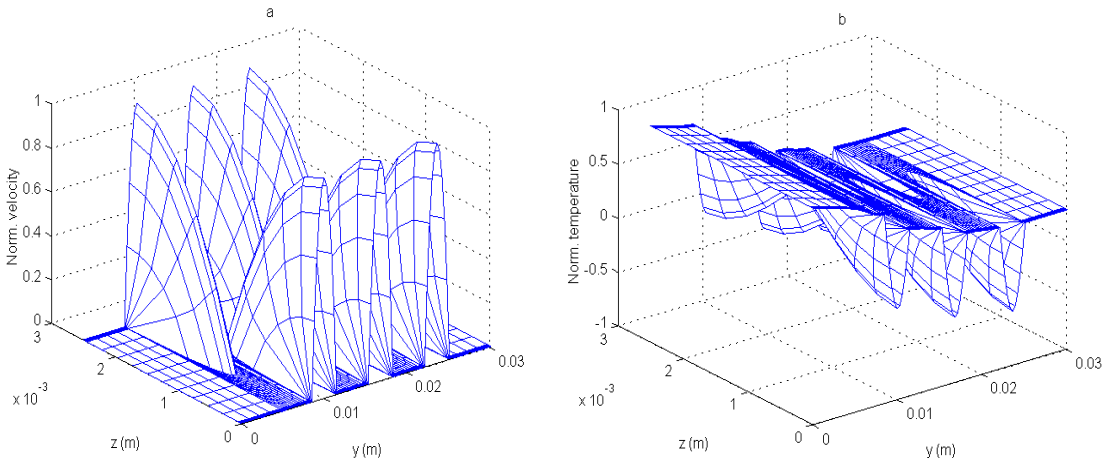

Fig. 5. Obtained normalized velocity (a) and temperature (b) distributions by constraining the channel diameter (be not smaller than 3 mm).

In Fig.6, the geometries are obtained by constraining the normalized hydraulic resistance ξ to be not higher than $1 \cdot 10^4$, $1 \cdot 10^3$, and 750. For the last case, the temperature distribution is shown in Fig. 7.

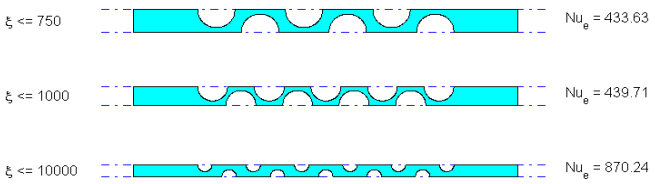

Fig. 6. Obtained optimum geometries by constraining the normalized hydraulic resistance (be not higher than $1 \cdot 10^4$, $1 \cdot 10^3$, and 750).

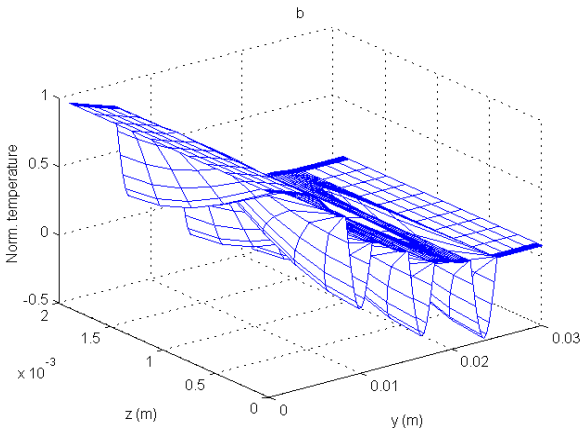

Fig. 7. Obtained normalized temperature distribution by constraining the normalized hydraulic resistance (be not higher than 750).

It is possible to observe that also under such a constraint the genetic algorithm tends to reach the limit values even if with some margins. These are probably due to the numerical discretization and a premature stop of the algorithm. Moreover, in respect of the optimum geometries that are obtained by

constraining the channel diameter, the geometries of Fig. 6 provide a 36.4 %, 93.5 %, and 95.1 % reduction in ξ with a 6.7 %, 52.9 %, and 53.5 % decrease in Nu_e, respectively. After observing the dependence of the optimized geometries on imposed constraints on the channel diameter and the hydraulic resistance, we can now propose a heat sink prototype that takes constructive needs into account. In particular, to produce cylindrical channels in an aluminium block with a 400 mm length easily, it is recommended to set the diameter not lower than 6.5 mm. Under such a constraint, the genetic algorithm gives the optimum geometry that is shown in Fig. 8. The corresponding temperature distribution is shown in Fig. 9.

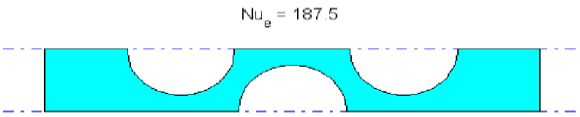

Fig. 8. Obtained optimum geometry for the hybrid solar panel prototype (D = 6.5 mm).

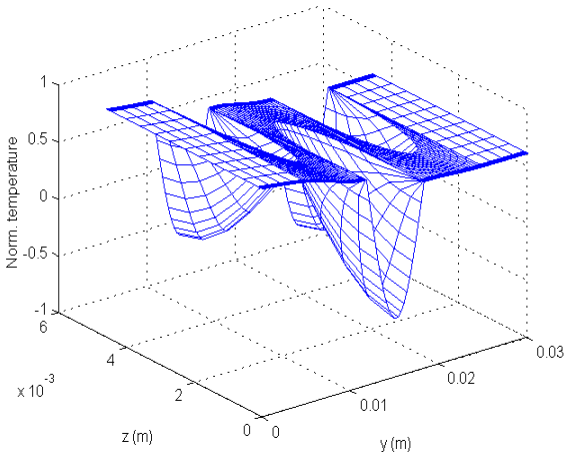

Fig. 9. Obtained normalized temperature distribution for the hybrid solar panel prototype (D = 6.5 mm).

Table 1. Values of Nu_e and ξ with subsequent optimizations.

Constrain	N	D [mm]	e [mm]	Nu_e	ζ
D >= 1 mm	11	1.0	1.0	933.70	$1.54 \cdot 10^4$
D >= 2 mm	7	2.0	1.5	622.59	$2.27 \cdot 10^3$
D >= 3 mm	5	3.0	2.6	444.53	$8.72 \cdot 10^2$
$\zeta <= 1 \cdot 10^4$	11	1.1	1.0	870.24	$9.79 \cdot 10^3$
$\zeta <= 1 \cdot 10^3$	9	2.3	1.5	439.71	$9.99 \cdot 10^2$
$\zeta <= 7.5 \cdot 10^2$	6	2.9	1.9	433.63	$7.48 \cdot 10^2$
D = 6.5 mm	3	6.5	4.6	187.52	$9.12 \cdot 10^6$

Different grids have been analyzed slightly; varying the number of knots aims to maintain a good result-related quality. By taking the 6 holes case into account as examples, Table 2 shows the obtained results.

Table 2. Six holes case results.

Lines	Columns	Delta Nu_e
21	79	Reference case
22	79	0.27 %
21	80	0.29 %

5. Conclusions

The obtained results showed that the performance of the heat sink that was employed in the proposed hybrid solar panel depended on a complex way on the number, the dimension, and the compactness of its channels. In particular, the best heat transfer effectiveness values could be obtained by setting the highest number of the smallest channels. Moreover, for given cross section areas for heat sink and channels, the setting of an additional channel increased convection and reduced conduction. Lastly, lower values can be obtained for the hydraulic resistance by compacting the channels or enlarging their diameter and reducing the heat transfer effectiveness in both cases.

References

[1] Dupré, O., Vaillon, R., & Green, M. A. (2015). Physics of the temperature coefficients of solar cells. *Solar energy materials and solar cells*, *140*, 92-100.

[2] Polman, A., & Atwater, H. A. (2012). Photonic design principles for ultrahigh-efficiency photovoltaics. *Nature materials*, *11*(3), 174.

[3] Michael, J. J., Iniyan, S., & Goic, R. (2015). Flat plate solar photovoltaic–thermal (PV/T) systems: a reference guide. *Renewable and sustainable energy reviews*, *51*, 62-88.

[4] Santbergen, R., & van Zolingen, R. C. (2008). The absorption factor of crystalline silicon PV cells: A numerical and experimental study. *Solar energy materials and solar cells*, *92*(4), 432-444.

[5] Santbergen, R. (2008). Optical absorption factor of solar cells for PVT systems (Doctoral dissertation, Eindhoven University of Technology). Retrieved from https://research.tue.nl/en/publications/optical-absorption-factor-of-solar-cells-for-pvt-systems

[6] Tripanagnostopoulos, Y., Nousia, T. H., Souliotis, M., & Yianoulis, P. (2002). Hybrid photovoltaic/thermal solar systems. *Solar energy*, *72*(3), 217-234.

[7] Charalambous, P. G., Kalogirou, S. A., Maidment, G. G., & Yiakoumetti, K. (2011). Optimization of the photovoltaic thermal (PV/T) collector absorber. *Solar energy*, *85*(5), 871-880.

[8] Garg, H. P., & Agarwal, R. K. (1995). Some aspects of a PV/T collector/forced circulation flat plate solar water heater with solar cells. *Energy conversion and management*, *36*(2), 87-99.

[9] Zondag, H. A., De Vries, D. W., Van Helden, W. G. J., Van Zolingen, R. J. C., & Van Steenhoven, A. A. (2003). The yield of different combined PV-thermal collector designs. *Solar energy*, *74*(3), 253-269.

[10] Zondag, H. A., de Vries, D. D., Van Helden, W. G. J., Van Zolingen, R. J. C., & Van Steenhoven, A. A. (2002). The thermal and electrical yield of a PV-thermal collector. *Solar energy*, *72*(2), 113-128.

[11] Tiwari, A., & Sodha, M. S. (2006). Performance evaluation of hybrid PV/thermal water/air heating system: a parametric study. *Renewable energy*, *31*(15), 2460-2474.

[12] Grefenstette, J. J. (1986). Optimization of control parameters for genetic algorithms. *IEEE transactions on systems, man, and cybernetics*, *16*(1), 122-128.

[13] Deb, K. (2014). Multi-objective optimization. *Search methodologies* (pp. 403-449). Springer, Boston, MA.

[14] Deb, K., Anand, A., & Joshi, D. (2002). A computationally efficient evolutionary algorithm for real-parameter optimization. *Evolutionary computation*, *10*(4), 371-395.

[15] Deb, K., Pratap, A., Agarwal, S., & Meyarivan, T. A. M. T. (2002). A fast and elitist multiobjective genetic algorithm: NSGA-II. *IEEE transactions on evolutionary computation*, *6*(2), 182-197.

[16] Farina, M., Deb, K., & Amato, P. (2004). Dynamic multiobjective optimization problems: test cases, approximations, and applications. *IEEE transactions on evolutionary computation*, *8*(5), 425-442.

[17] Peigin, S., Epstein, B., & Gali, S. (2004). Multilevel parallelization strategy for optimization of aerodynamic shapes. *Parallel computational fluid dynamics 2003*, 505-512.

[18] Queipo, N., Devarakonda, R., & Humphrey, J. A. C. (1994). Genetic algorithms for thermosciences research: application to the optimized cooling of electronic components. *International journal of heat and mass transfer*, *37*(6), 893-908.
[19] Peng, H., & Ling, X. (2008). Optimal design approach for the plate-fin heat exchangers using neural networks cooperated with genetic algorithms. *Applied thermal engineering*, *28*(5-6), 642-650.
[20] Chow, T. T., Zhang, G. Q., Lin, Z., & Song, C. L. (2002). Global optimization of absorption chiller system by genetic algorithm and neural network. *Energy and buildings*, *34*(1), 103-109.
[21] Gosselin, L., Tye-Gingras, M., & Mathieu-Potvin, F. (2009). Review of utilization of genetic algorithms in heat transfer problems. *International journal of heat and mass transfer*, *52*(9-10), 2169-2188.
[22] Azarkish, H., Sarvari, S. M. H., & Behzadmehr, A. (2010). Optimum design of a longitudinal fin array with convection and radiation heat transfer using a genetic algorithm. *International journal of thermal sciences*, *49*(11), 2222-2229.
[23] Sanaye, S., & Hajabdollahi, H. (2010). Thermal-economic multi-objective optimization of plate fin heat exchanger using genetic algorithm. *Applied energy*, *87*(6), 1893-1902.
[24] Najafi, H., Najafi, B., & Hoseinpoori, P. (2011). Energy and cost optimization of a plate and fin heat exchanger using genetic algorithm. *Applied thermal engineering*, *31*(10), 1839-1847.
[25] Das, R. (2012). Application of genetic algorithm for unknown parameter estimations in cylindrical fin. *Applied soft computing*, *12*(11), 3369-3378.
[26] Amini, M., & Bazargan, M. (2014). Two objective optimization in shell-and-tube heat exchangers using genetic algorithm. *Applied thermal engineering*, *69*(1-2), 278-285.
[27] Patel, V. K., & Savsani, V. J. (2015). Heat transfer search (HTS): a novel optimization algorithm. *Information sciences*, *324*, 217-246.
[28] Wen, J., Yang, H., Tong, X., Li, K., Wang, S., & Li, Y. (2016). Configuration parameters design and optimization for plate-fin heat exchangers with serrated fin by multi-objective genetic algorithm. *Energy conversion and management*, *117*, 482-489.
[29] Biyanto, T. R., Gonawan, E. K., Nugroho,nG., Hantoro, R., Cordova, H., & Indrawati, K. (2016). Heat exchanger network retrofit throughout overall heat transfer coefficient by using genetic algorithm. *Applied thermal engineering*, *94*, 274-281.
[30] Khan, T. A., & Li, W. (2017). Optimal design of plate-fin heat exchanger by combining multi-objective algorithms. *International journal of heat and mass transfer*, *108*, 1560-1572.
[31] Fabbri, G. (1997). A genetic algorithm for fin profile optimization. *International journal of heat and mass transfer*, *40*(9), 2165-2172.
[32] Fabbri, G. (1998). Optimization of heat transfer through finned dissipators cooled by laminar flow. *International journal of heat and fluid flow*, *19*(6), 644-654.
[33] Fabbri, G., Greppi, M., & Lorenzini, M. (2012). Optimization with genetic algorithms of PVT system global efficiency. *Journal of energy and power engineering*, *6*(7), 1035.